NANOMEDICINE

# Drug-eluting microfibrous patches for the local delivery of rolipram in spinal cord repair

Timothy L. Downing [a,b,1], Aijun Wang [b,1,2], Zhi-Qiang Yan [c], Yvette Nout [d,3], Andy L. Lee [b], Michael S. Beattie [d], Jacqueline C. Bresnahan [d], Diana L. Farmer [e], Song Li [a,b,*]

[a] UC Berkeley & UCSF Joint Graduate Program in Bioengineering, Berkeley/San Francisco, CA, USA
[b] Department of Bioengineering, University of California, Berkeley, B108A Stanley Hall, Berkeley, CA 94720-1762, USA
[c] Institute of Mechanobiology & Medical Engineering, Shanghai Jiao Tong University, Shanghai, China
[d] Brain and Spinal Injury Center, Department of Neurological Surgery, University of California, San Francisco, USA
[e] Department of Surgery, University of California, Davis, School of Medicine, Sacramento, CA 95817, USA

## ABSTRACT

Spinal cord injury (SCI) remains a major challenge for regenerative medicine. Following SCI, axon growth inhibitors and other inflammatory responses prevent functional recovery. Previous studies have demonstrated that rolipram, an anti-inflammatory and cyclic adenosine monophosphate preserving small molecule, improves spinal cord regeneration when delivered systemically. However, more recent studies showed that rolipram has some adverse effects in spinal cord repair. Here, we developed a drug-delivery platform for the local delivery of rolipram into the spinal cord. The potential of drug-eluting microfibrous patches for continuous delivery of high and low-dose rolipram concentrations was characterized in vitro. Following C5 hemisections, athymic rats were treated with patches loaded with low and high doses of rolipram. In general, animals treated with low-dose rolipram experienced greater functional and anatomical recovery relative to all other groups. Outcomes from the high-dose rolipram treatment were similar to those with no treatment. In addition, high-dose treated animals experienced reduced survival rates suggesting that systemic toxicity was reached. With the ability to control the release of drug dosage locally within the spinal cord, drug-eluting microfibrous patches demonstrate the importance of appropriate local release-kinetics of rolipram, proving their usefulness as a therapeutic platform for the study and repair of SCI.

© 2012 Elsevier B.V. All rights reserved.

## 1. Introduction

Spinal cord repair remains one of the biggest challenges for regenerative medicine. Recent studies have found that spinal cord injury (SCI) is over five times more prevalent than previously estimated, bringing the total number of people living with SCI to over one million in the United States alone [1]. In addition, as palliative care continues to advance, this number will continue to rise.

Severe SCI is marked by a disruption in the ascending and descending axons of the spinal tracts. This disruption prevents vital communication between the brain and other parts of the body. Following injury, neural cells die—namely neurons and oligodendrocytes; molecules that are inhibitory to axon growth are secreted; and reactive astrocytes and infiltrating macrophages facilitate glial scar formation, leading to the physical and chemical impedances of axon growth [2–7]. These events are accompanied by active secondary degeneration of myelin tissues, causing additional losses in neural cell populations at or near the injury site [8,9]. Together, these events cause paralysis and prevent natural recovery. Considering this, a successful regenerative strategy might require a combination of therapies that have independently been shown to mitigate the previously mentioned pathophysiologies. Before such a strategy can become a reality, however, the efficacy and safety of each individual therapy must be ensured.

Previous research has demonstrated the therapeutic utility of small molecule drugs such as rolipram in spinal cord repair [7,10]. With its anti-inflammatory [11,12] and cyclic adenosine monophosphate preserving properties, rolipram has been shown to promote regeneration of new axons [13,14], aid in the preservation of myelinated tissues [15], attenuate acute oligodendrocyte death [16,17], reduce reactive gliosis and subsequent glial scar formation [14], and significantly improve functional recovery [13,14,17,18] after SCI. However, more recent studies have presented data that leave the efficacy and safety of rolipram usage for spinal cord repair in question.

* Corresponding author at: Department of Bioengineering, University of California, Berkeley, B108A Stanley Hall, Berkeley, CA 94720-1762, USA. Tel.: +1 510 666 2799; fax: +1 510 666 3381.
*E-mail address:* song_li@berkeley.edu (S. Li).
[1] Contributed equally to this work.
[2] Present address: Department of Surgery, University of California, Davis, School of Medicine, Sacramento, CA 95817, USA.
[3] Present address: Department of Animal and Veterinary Sciences, College of Agriculture, California State Polytechnic University, Pomona, CA 91768, USA.

A study led by Sharp et al. was unable to replicate the beneficial effects observed through the subcutaneous (s.c.) delivery of rolipram in combination with the transplantation of Schwann cells as previously reported by Pearse et al. [19]. A second report also found little added functional recovery from the systemic delivery of rolipram with the transplantation of a glial restricted precursor cell population [20]. Interestingly, the latter report also suggested that the s.c. delivery of rolipram could lead to adverse effects locally within the spinal cord (e.g., increased death of transplanted cells) as well as systemically (e.g., increased body-weight loss and micturition peak frequencies). While others have reported the importance of the local concentration of rolipram within the spinal cord [14], the conflict surrounding rolipram usage for spinal cord repair remains largely unresolved.

Several groups have utilized biodegradable scaffolds for many neural regeneration strategies [21–29]. Previously we have explored the use of natural materials [30] and synthetic scaffolds with and without drug-delivery for spinal cord regeneration [31,32]. Electrospun nanofibrous patches, with rolipram immobilized to the surface via hydrophobic adsorption, showed anatomical as well as functional improvements after a T9–T11 level SCI. The direct combination of rolipram with the fibrous topography of patches was shown to increase axon growth through the membrane and in the lesion, promote angiogenesis through the membrane, and decrease the population of astrocytes and chondroitin sulfate proteoglycans at the lesion [31]. However, with only the adsorption of rolipram onto fibrous patches via hydrophobic interactions, very little control over drug loading and subsequent release-kinetics was achieved. A new platform with greater control over the local delivery of small molecule drugs into the spinal cord would greatly assist in better understanding the effects of rolipram dosage in spinal cord repair, ultimately allowing for the development of more robust therapeutic strategies.
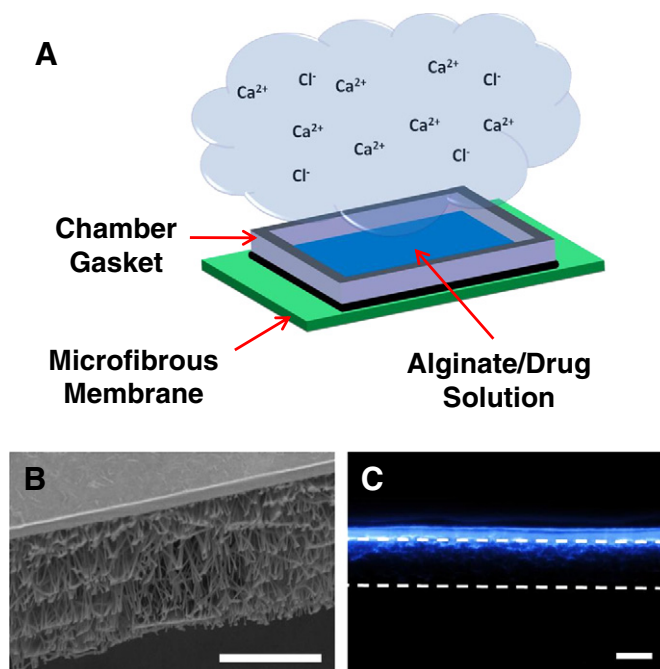
## 2. Materials and methods

### 2.1. Microfibrous membrane fabrication

The assembly of drug-eluting microfibrous patches began with the fabrication of biodegradable microfibrous membranes. Electrospinning technology was employed for this purpose as previously described [25,33]. Briefly, a polymer solution composed of 19% (w/v) poly(L-lactide), M.W. 85,000–160,000 (PLLA, Sigma) dissolved in 1-1-1,3-3-3 hexafluoro-2-propanol (Matrix Scientific) was jetted from an electrically charged (12 kV) single-needle spinneret and collected onto a grounded rotating mandrel (800 RPM; 10 cm diameter). The electrospinning distance was fixed at 7 cm. Once formed, membranes where submerged in water at 65 °C and mechanically stretched to further induce fiber alignment. For decontamination, membranes were submerged in 70% ethanol for 30 min and thoroughly washed in sterile PBS.

### 2.2. The assembly and characterization of drug-eluting microfibrous patches

PRONOVA™ Ultrapure LVM sodium alginate (NovaMatrix™; FMC BioPolymer) was used to form a thin hydrogel layer on top of microfibrous membranes. This hydrogel layer was used as a drug excipient for the local delivery of rolipram into the spinal cord. Removable polystyrene chamber gaskets were modified from Lab-Tek™ II Chamber Slide™ Systems (Thermo Scientific). Chamber gaskets were placed on top of microfibrous membranes and secured, creating a 2 cm by 2 cm well for hydrogel placement (Fig. 1A). Five-hundred microliters of a 2% (w/v) sodium alginate solution, dissolved in deionized (d.i.) water, was added to chamber wells and layered over each membrane surface. In order to obtain a flat and homogenously polymerized hydrogel, this sodium alginate layer was crosslinked using a calcium chloride-rich



**Fig. 1.** Assembly and structure of drug-eluting microfibrous patches. (A) A schematic illustrating the assembly of drug-eluting microfibrous patches. Chamber gasket is used to create a well for sodium alginate solution (loaded with drug or empty) placement over the top of PLLA microfibrous membranes. In addition, a novel calcium chloride-rich mist crosslinking mechanism is demonstrated. SEM image reveals (B) the structure of microfibrous membrane and alginate layers within drug-eluting microfibrous patches. (C) Fluorescent micrograph of patch cross-section shows the incorporation of small fluorescent molecules (DAPI) into the alginate layer. Dashed lines indicate microfibrous membrane boundaries. Scale bars = 50 μm.

mist. Mist was produced via ultrasonic vibrations generated by a Nutramist™ 3-head fog module (FutureGarden™). Following crosslinking, newly formed alginate hydrogels were air-dried onto microfibrous membrane surfaces at 37 °C overnight and chamber gaskets were removed. This process helped to slow the elution of loaded drugs during rehydration [34] as well as reduce patch thickness for implantation. The microscale structure of drug-eluting microfibrous patches was resolved under high-powered scanning electron microscopy (SEM). Microfiber diameter typically ranged from 500 nm to 1 μm; however, fiber diameters up to 2 μm were occasionally observed.

### 2.3. Rolipram loading concentration and drug-release profile

Drug-eluting microfibrous patches were loaded with variable concentrations of rolipram. To do so, rolipram was first dissolved in DMSO (0.1 mg/μl) and then added to a larger volume of d.i. water. An equal volume of 4% sodium alginate was then added to rolipram solutions, bringing the final sodium alginate concentration to 2%. Final concentrations of rolipram were 25 (low-dose) and 500 (high-dose) μg/ml. The final amounts of DMSO within hydrogels were ≤0.5% (vol/vol). To minimize the risk of contamination, patches were fabricated under sterile conditions in a laminar airflow hood. In addition, all materials and devices used were decontaminated with 70% ethanol and solutions were sterile-filtered through a 0.2 μm filter prior to use.

To obtain the release profiles of rolipram, drug-eluting microfibrous patches were made by using either 100 or 500 μl of rolipram-loaded sodium alginate. After fabrication, patches were submerged in 0.5 ml of PBS and incubated at 37 °C for up to 14 days. At selected time points (18 h; 1.5, 3, 7, and 14 days) solution was withdrawn and the amount of rolipram in the withdrawn solution was determined via HPLC. From this information the total amount of released rolipram was calculated and release profiles were generated.

## 2.4. Cervical spinal cord hemisection and subdural patch implantation

All experimental procedures with animals were approved by the ACUC committee at UC Berkeley and were carried out according to the institutional guidelines. All efforts were made to minimize the number of animals used and their suffering. Adult female athymic rats (National Cancer Institute) weighing 170–243 g were used in all experiments. Four experimental groups were included: hemisection injury with (1) no patch or treatment (untreated), (2) empty drug-eluting microfibrous patch treatment (blank patch), (3) low-dose rolipram patch treatment (low-dose rolipram), and (4) high-dose rolipram patch treatment (high-dose rolipram).

Drug-eluting microfibrous patches were implanted subdurally for the direct delivery of rolipram to the spinal cord. Laminectomies were performed on the fourth through sixth cervical vertebrae, exposing the spinal cord at the desired lesion site. The dura was opened with a single longitudinal incision approximately 0.5 cm in length. A fine scalpel blade was used to create spinal cord hemisection lesions moving outward starting from the midline. This lesion only caused damage on the right side of the spinal cord. Each injury was inspected to ensure the complete severance of spinal cord tissues above and below the lesion site. Additional damage to the dura was avoided. Before implantation, patches were trimmed down to an appropriate size (0.5 cm by 0.3 cm). Patches were then carefully implanted underneath the dura, insuring that the hydrogel layer faced medially toward the injury site. The dura was then sutured closed over implanted patches using 9–0 sutures. Untreated animals received no additional therapy and the dura was closed immediately after hemisection. In all cases, the surgery site was closed in multiple layers.

## 2.5. Forelimb motor assessment

In order to assess the degree of animal functional motor recovery after cervical SCI we utilized the open-field forelimb recovery rating scale as previously described [35,36]. Briefly, at various time points post injury (2 days; 1, 2, 3, 4, 6, and 8 weeks) animals were placed in a circular foam-enclosed arena (100 cm diameter, 40 cm wall height) and scored. Scoring was separated into six major categories: articular movement of the shoulder (2), elbow (2), and wrist (2); stationary (2) and active (2) weight support; digit position (2); stepping (6); forelimb–hindlimb coordination (3); and tail position (1); (note: parenthesis denotes point totals for each category). Scores were summed to obtain an overall Martinez forelimb score (20 points max). All rats were scored over a 4 minute time window, and all scorers were blind to the animals' experimental group. Open-field sessions were video recorded for score accuracy confirmation.

## 2.6. Histopathology and immunohistochemistry

Eight weeks after spinal cord hemisections, animals were sacrificed and immediately perfused with 4% paraformaldedyde (PFA). The C2–C7 segment of rat spinal cords was explanted and kept in 4% PFA at 4 °C for 24 h and later cryoprotected in 30% sucrose in PBS. Cross sections of the spinal cord, through the lesion site, were cryosectioned (10 μm in thickness) for H&E (hematoxylin and eosin) staining and immunostaining. Spinal cord cross sections were immunostained for the following: neurofilament (NFM, rabbit polyclonal antibody, Sigma-Aldrich) to identify axons, myelin basic protein (MBP, rabbit polyclonal antibody, Sigma-Aldrich) for oligodendrocyte myelin, and glial fibrillary acidic protein (GFAP, rabbit polyclonal antibody, Millipore) for reactive astrocytes. For chondroitin sulfate proteoglycan (CSPG, mouse monoclonal antibody, Sigma-Aldrich) identification, slides were kept in 10 mM sodium citrate buffer (pH 6.0) at 95–99 °C for 10 min for antigen retrieval before the immunostaining procedure was performed. For fluorescence signal intensity quantification, multiple images within the lesion sites of animals from each group were captured and a threshold of intensity was defined to identify proteins of interest. ImageJ software was then used to calculate the average total pixels per image for NFM, MBP, GFPA and CSPG marker expression.

## 2.7. Statistical analysis

All data are presented as mean ± standard deviation. Data from behavioral scores, where time and treatment vary, were analyzed using a two-way analysis of variance (ANOVA) with repeated measures. Differences between groups were determined using Tukey's post-hoc test. A one-way ANOVA was used to analyze in vitro release profiles and average total pixel quantifications. Survival data were analyzed using a log-rank (Mantel–Cox) test where the survival curve of each treatment group was compared to that of untreated animals. Linear regression analysis was performed on animal weight loss over time to determine if slopes varied significantly from zero. For all cases, p-values less than 0.05 were considered statistically significant. GraphPad Prism® 5.0 software was used for all statistical evaluations.
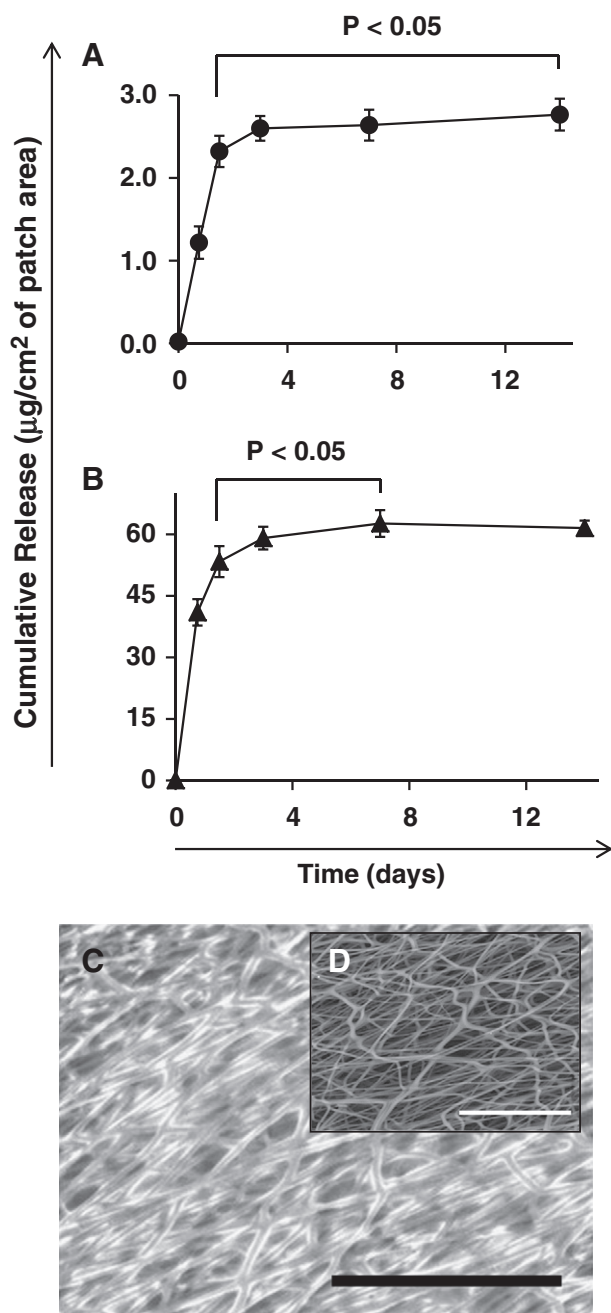
## 3. Results

### 3.1. Structure and appearance of drug-eluting microfibrous patches

We used electrospinning technology to produce biodegradable PLLA microfibrous membranes. Membranes were mechanically stretched to induce fiber alignment. After membranes were fabricated, a thin alginate hydrogel layer was formed on top. SEM revealed the intimate juxtaposition of the highly aligned microfibrous membrane and thin alginate hydrogel layer (Fig. 1B)—with fibers extending outward with respect to the plane of the captured image. Fluorescence microscopy confirmed the ability of drug-eluting microfibrous patches to encapsulate small fluorescent molecules (4′,6-diamidino-2-phenylindole, DAPI) within their thin hydrogel layer (Fig. 1C). Membrane thickness ranged from 50 to 100 μm and the dried alginate hydrogel layer typically added an additional 5.3 μm in thickness. After rehydration, hydrogel thickness was approximately 20 μm.

### 3.2. Controlled release of rolipram from drug-eluting microfibrous patches

Drug-eluting microfibrous patches were loaded with low-dose or high-dose concentrations of rolipram (3.1 and 62.5 μg/cm$^2$, respectively) and the subsequent in vitro release profiles were observed (Fig. 2A, B). The low-dose concentration of rolipram (in amount per unit area) was consistent with our previous SCI study where rolipram-loaded patches significantly enhanced spinal cord regeneration [31]. The high-dose concentration was chosen as an upper limit for drug loading capacity as to not compromise alginate's gelation properties. As expected, high-dose rolipram patches delivered approximately 20 fold more drug than low-dose rolipram patches. It is important to note that nearly 10% of loaded rolipram remained unreleased in low-dose rolipram patches after 14 days, leaving the possibility of additional drug release. Release profiles showed that drug-eluting microfibrous patches were capable of maintaining a significant release of rolipram beyond 1.5 days over a wide range of loading concentrations. Furthermore, low-dose rolipram patches exhibited an 18-hour burst release of 38.7% while high-dose rolipram patches showed a burst release of 65.6%. Both conditions demonstrated significant improvements over our previous drug-delivery platform which, through the passive adsorption of rolipram, displayed a 4-hour burst release of over 90% [31]. It is also worth noting that patches retained residual amounts of their hydrogel layer after 12 days at 37 °C in PBS. SEM reveals the structure of this residual

**Fig. 2.** Low and high-dose rolipram in vitro release profiles. Cumulative release profiles of low (A) and high-dose (B) rolipram patches at 37 °C in PBS. Statistical analysis shows that a significant amount of rolipram was released beyond 1.5 days for both cases. SEM image reveals (C) residual alginate hydrogel on microfibrous membrane surface after 12 days at 37 °C in PBS. (D) SEM image of bare microfibrous membrane surface for comparison. Scale bar = 50 μm.

blank patch; a low-dose rolipram patch, or a high-dose rolipram patch. Fig. 3 illustrates the implantation of patches post SCI.

In general, animals treated with empty patches experienced modest improvement over untreated animals. When animals were treated with low-dose rolipram patches we observed drastic improvements in functional outcomes. Specifically, Martinez forelimb open-field scores showed that animals treated with low-dose rolipram patches (n = 3) score significantly higher, from weeks 1 through 4, 6 and 8, when compared to all other animals (Fig. 4A). In contrast, animals treated with patches loaded with 20 times more rolipram (high-dose rolipram; n = 4) showed no significant differences with respect to untreated animals (n = 4). Statistical significance of open-field score differences was assessed using a two-way ANOVA.

Articular movement scores show early motor improvements for low-dose rolipram-treated animals. During the first week of this study, these animals displayed significantly more range-of-motion in forelimb joints (e.g., shoulder, elbow, and wrist). Fig. 4B shows animal forelimb articular movement scores at 2 day and 1 week time points. After 1 week, low-dose rolipram-treated animals scored significantly higher than all other groups. No other scores were significantly different.

During week 8 of this study, animal forelimb–hindlimb coordination frequencies were observed (Fig. 4C). Sixty-seven and thirty-three percent of rats treated with low-dose rolipram patches experienced "consistent" and "frequent" coordination behaviors, respectively. Animals in other groups experienced no consistent coordination at all. Twenty-five percent of rats treated with empty patches (n = 4) showed frequent



**Fig. 3.** Implantation of drug-eluting microfibrous patches after SCI. (A) Schematic of subdural implantation of drug-eluting microfibrous patches into the injured cord. (B) Macroscopic view of the lesion site and patch during animal surgery. An asterisk was used to mark the location of the drug-eluting microfibrous patch. (C, D) Gross histology of spinal cord cross section 8 weeks post SCI. H&E staining reveals new tissue formation at the lesion site and patch's ability to integrate into the surrounding tissues (D). (C) Less regenerated control for comparison. Here, arrows point to the implantation site for drug-eluting microfibrous patches. Black dashes outline areas of less tissue formation for comparison.

hydrogel layer relative to the membrane's bare surface (Fig. 2C, D, respectively).

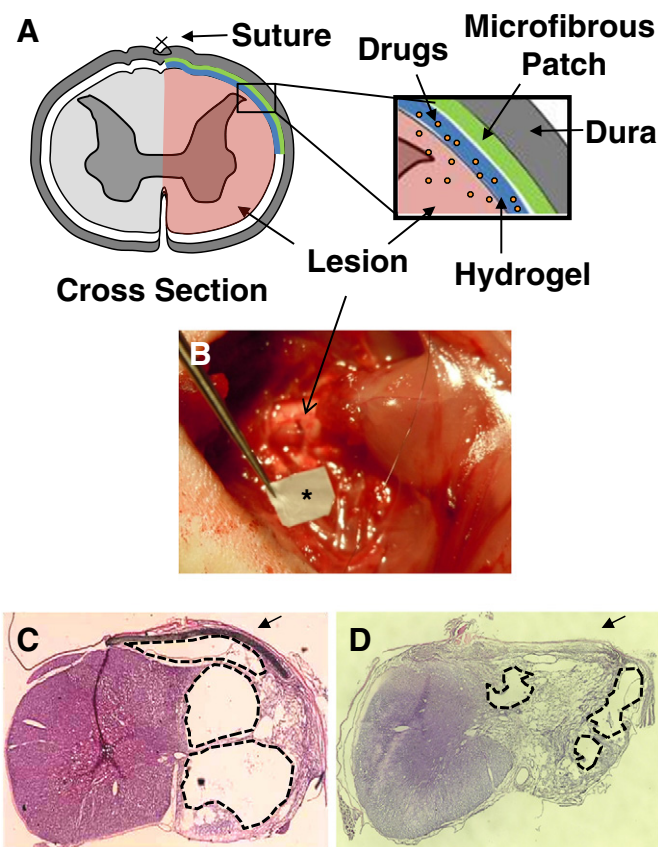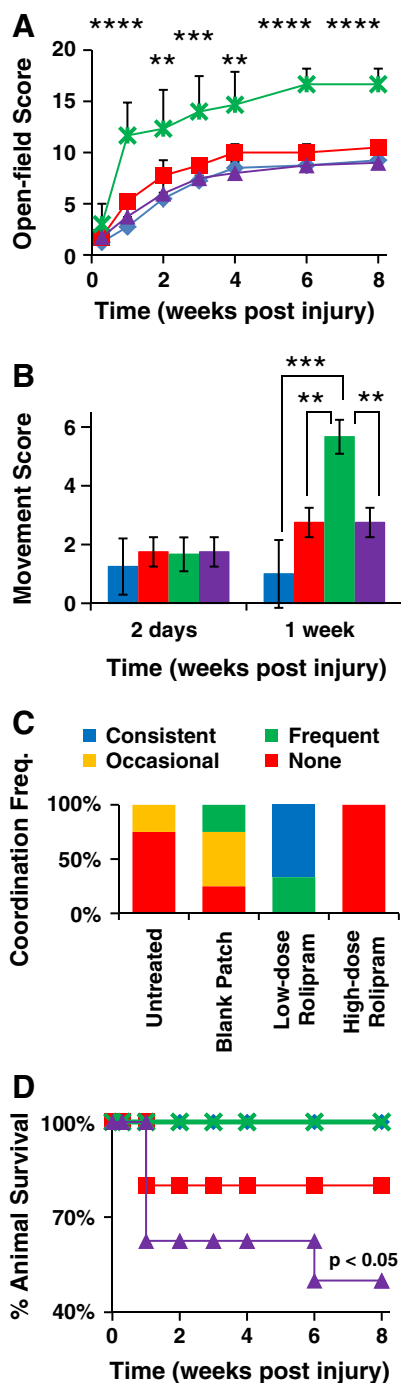### 3.3. Effect of local and low-dose rolipram on forelimb recovery

To assess the therapeutic utility of drug-eluting microfibrous patches for the study and repair of SCI, rats were subjected to a C5 hemisection lesion. Immediately after injury, animals were either left untreated or given one of three drug-eluting microfibrous patches: a

**Fig. 4.** Functional recovery of forelimb locomotion based on the Martinez recovery scale and animal survival. (A, B, D) Scoring was performed across four groups: untreated (blue, -♦-), blank patch (red, -■-), low-dose rolipram patch (green, -X-), and high-dose rolipram patch (purple, -▲-). (A) Overall Martinez open-field scores from weeks 1 through 4, 6 and 8. Asterisks indicate where low-dose rolipram scores were significantly greater than all other animals (****, ***, and ** denote p<0.0001, 0.001, and 0.01, respectively). (B) Forelimb articular movement scores at 2 days and 1 week post SCI (*** and ** denote p<0.001 and 0.01, respectively). (C) Animal forelimb–hindlimb coordination frequency at 8 weeks post SCI. (D) Animal survival over the course of 8 weeks following the initial SCI. A log-rank (Mantel–Cox) test was used to determine significance.

### 3.4. Effects of high-dose rolipram on animal survival

At the completion of this study we reviewed animal survival data in an effort to assess overall animal health (Fig. 4D). Upon the recommendation of unbiased veterinary experts, animals were sacrificed for various health-related reasons. These included excessive weight-loss, self-mutilation, and poor general health. For untreated animals and animals treated with blank and low-dose rolipram patches, animal survival rates ranged from 80 to 100%. Animals treated with high-dose rolipram patches showed a drastic drop off in survival rate (50%). Statistical analysis reveals that this survival curve is significantly (p<0.05) different than that of untreated animals. Although most animal deaths were sacrificial, one animal within the high-dose rolipram group was found deceased in its cage at week 6. There were no other cases where animal death was observed beyond the first week. To confirm this apparent increase in toxicity, we performed an analysis on animal weight loss over days 3 through 6 after SCI (Supplemental Fig. 1). From this analysis, we confirmed that high-dose treated animals continued to experience significantly (p<0.05) more weight loss within the first week.

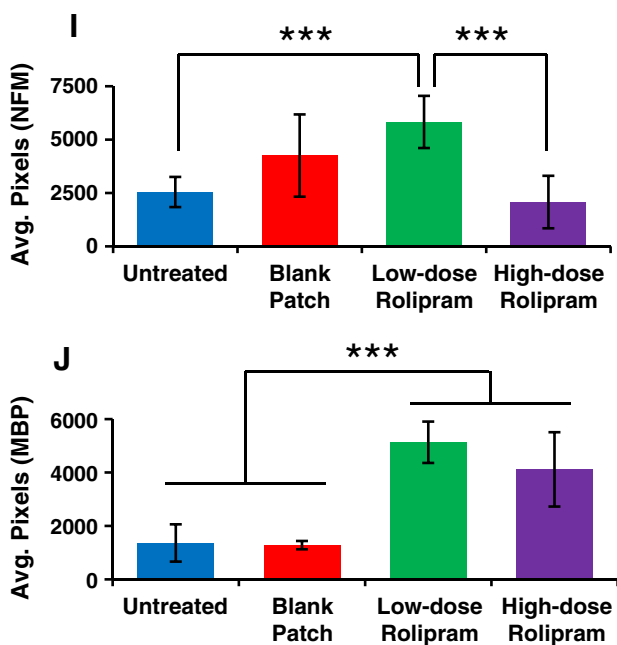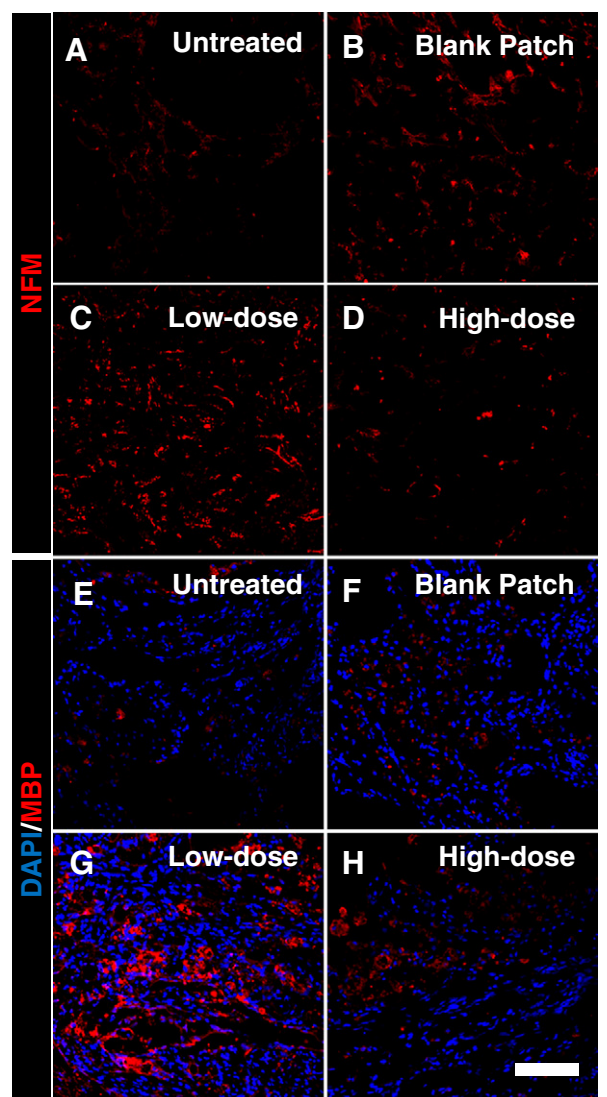### 3.5. Gross histopathology and anatomical improvement

Eight weeks after initial injuries, rats were sacrificed and immunohistological analyses were performed on spinal cord tissues and patches. Spinal cord sections from each experimental group were stained for NFM (Fig. 5A–D), MBP (E–H), GFAP (Fig. 6A–D), and CSPG (E–H). Figs. 5 and 6 illustrate the representative trends observed across all stains. In general, animals treated with blank patches commonly showed slightly more axon outgrowth (indicated with NFM immunostaining) into the lesion site when compared to untreated animals. Furthermore, animals treated with low-dose rolipram patches exhibited the greatest degree of axon outgrowth into the lesion site when compared to all other groups. Animals treated with high-dose rolipram patches showed a drastic decrease in the number of axons present when compared to low-dose rolipram and blank patch treated animals.

A similar trend was observed regarding the presence of oligodendrocyte cell (MBP$^+$) populations within the injury site after low-dose rolipram delivery. Specifically, immunostained sections for animals treated with low-dose rolipram patches showed an increase in the number of MBP$^+$ cells with respect to all other groups (Fig. 5E–H), suggesting the enhancement of myelin formation and/or sparing of oligodendrocytes. Fig. 5I and J attempts to quantitatively represent the degree of anatomical recovery seen in axon outgrowth and oligodendrocyte myelin, respectively.

As expected, animals left untreated showed a substantial number of reactive astrocytes present within their lesion sites (Fig. 6A). The application of any type of patch seemed to reduce the number of astrocytes seen at the lesion (Fig. 6B–D). While high-dose treatment produced a significant decrease in the number of astrocytes present, low-dose treatment resulted in the most dramatic decrease (Fig. 6I). After analyzing extracellular matrix components within cord lesions we found that animals treated with low-dose rolipram patches had no significant change in CSPG content at their lesion site relative to animals from untreated and blank patch groups (Fig. 6E–G). Interestingly, animals treated with high-dose rolipram patches showed a dramatically higher CSPG content (Fig. 6H) within their lesions compared to low-dose treated and untreated animals (Fig. 6J).

## 4. Discussion

Many studies have outlined the beneficial role that rolipram can have in spinal cord repair. However, recent studies suggest that its s.c. delivery may lead to systemic toxicity and less robust functional recovery [20,37]. Fig. 7 attempts to illustrate the concerns and potential

coordination and another 50% showed "occasional" coordination, leaving 25% with no coordination. Untreated animals remained mostly (75%) uncoordinated. Animals treated with high-dose rolipram-loaded patches showed no coordination whatsoever.
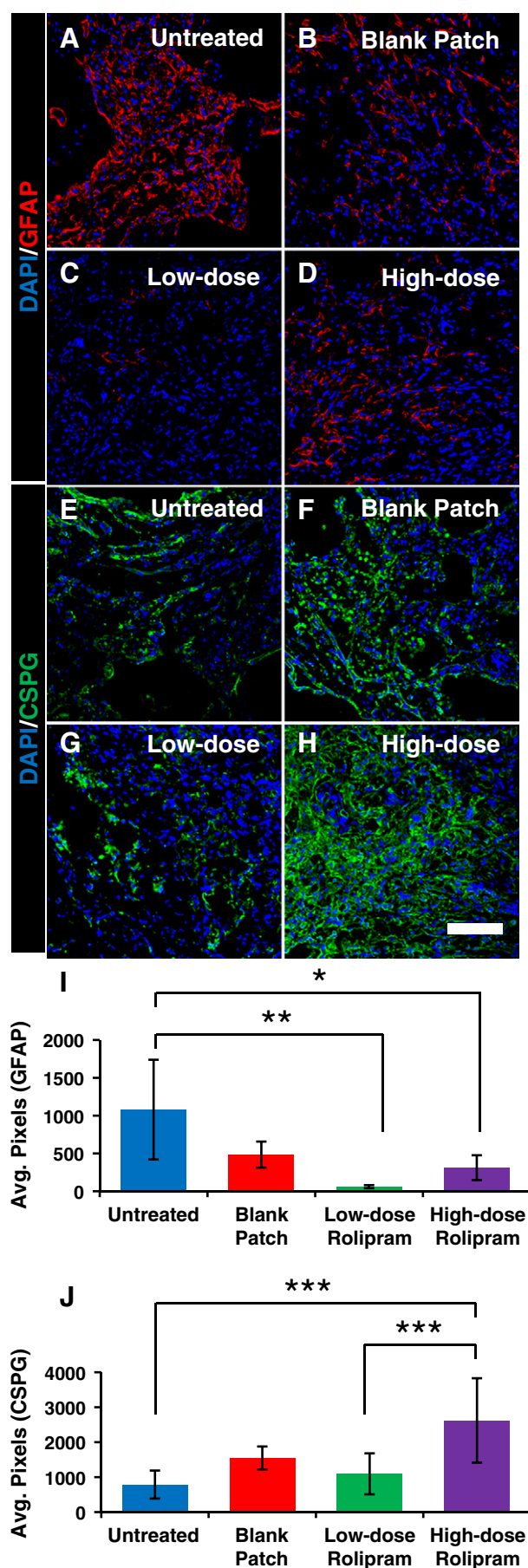
pitfalls that may complicate the usage of rolipram through s.c. injections for spinal cord repair. Achieving an optimal concentration of rolipram within the spinal cord requires a complicated balance of minimizing systemic toxicity, avoiding spinal cord over-dosage, and appropriately accounting for patient/injury variations. Furthermore, the co-delivery of other therapeutic agents (i.e., transplanted cells) may further convolute this balance [38]. Conceptually, this may help to explain conflicting results found by previous studies. For example, while Pearse et al. [13] demonstrated significant spinal cord recovery after systemic delivery of rolipram, they also reported that "rats treated with rolipram showed increased secretion of porphyrin from the eyes" indicating that some degree of toxicity was reached. Under nearly identical experimental conditions, Sharp et al. [19] found that rolipram offered no additional recovery over untreated animals. Using similar experimental conditions, Nout et al. [20] showed that systemic delivery of rolipram offered little functional recovery over untreated animals and resulted in significant reductions in animal health. Interestingly, Nikulina et al. [14] found that rolipram offered improvements in recovery when delivered at a rate approximately 10 times greater than the previously mentioned studies. Even more, there was evidence that even higher dosages can yield local toxicity within the injured cord (e.g., less regeneration). This study was, however, done using a different injury model (e.g., hemisection versus contusion) and different rat strains and, therefore, may be difficult to compare. Given these conflicting results and the fact that the local rolipram concentration within the spinal cord is often unknown or unreported, we are unable to definitively determine specific systemic dosages that are therapeutic versus toxic. Still, these results, considered together, highlight the variability that s.c. delivery of rolipram brings to spinal cord repair.

In an effort to avoid the complications observed with the s.c. delivery of rolipram, we attempted to create a new and improved platform that would allow for controlled, local drug-delivery into the spinal cord. With the incorporation of an alginate hydrogel layer as a drug excipient, drug-eluting microfibrous patches successfully demonstrated their ability to 1) suppress the extent of burst release previously seen with our small molecule drug-delivery devices and 2) sustainably deliver rolipram beyond 1.5 days in vitro over a large range of drug loading concentrations. Several studies demonstrate rolipram's efficacy even when delivered acutely (3 days or less) [16,18,39]. Given this, we felt our patches were suitable for in vivo experimentation. While our previous spinal cord patch fabrication utilized blends of PLLA and poly(D,L-lactide-co-glycolide) (PLGA), here patches were composed of only PLLA polymer to reduce the potential influence of acidic polymer contaminants due to the rapid degradation of PLGA. Consistent with our previous result [31], drug-eluting microfibrous patches loaded with a low-dose (3.1–3.9 μg/cm$^2$) concentration of rolipram facilitated the greatest degree of animal functional and anatomical recovery. In particular, improvements in overall forelimb recovery as well as early forelimb joint movement were greater for animals treated with a low dosage of rolipram. Anatomical improvements included increases in the number of both axons and oligodendrocytes seen within the lesion site. In addition, a decrease in the number of reactive astrocytes and the amount of CSPG molecules present were observed. For most outcomes, patches loaded with a high-dose concentration of rolipram appeared to have little variation from the no treatment case. Interestingly, CSPG content within lesions, however, was much higher for animals treated with a high dosage of rolipram. In addition, high-dose rolipram-treated animals

Fig. 5. Histological analysis of NFM and MBP staining at 8 weeks post SCI. Representative immunofluorescent staining of tissue regeneration within the lesion site of spinal cord cross sections in untreated animals (A, E), blank patch treated animals (B, F), low-dose rolipram-treated animals (C, G), and high-dose rolipram-treated animals (D, H). Axons in the lesion were identified using NFM antibodies (A–D). Oligodendrocyte myelin was identified using MBP antibodies (E–H). DAPI staining was used to identify cell nuclei. Scale bar = 100 μm. (I, J) ImageJ software was used to quantify the average total pixels for NFM$^+$ axons or MBP$^+$ oligodendrocytes, respectively, within immunostained sections.

**Fig. 6.** Histological analysis of GFAP and CSPG staining at 8 weeks post SCI. Representative immunofluorescent staining of tissue regeneration within the lesion site of spinal cord cross sections in untreated animals (A, E), blank patch treated animals (B, F), low-dose rolipram-treated animals (C, G), and high-dose rolipram-treated animals (D, H). Astrocytes in the lesion were identified by GFAP antibody staining (A–D). Glial scar formation was identified using CSPG antibodies (E–H). DAPI staining was used to identify cell nuclei. Scale bar = 100 μm. (I, J) ImageJ software was used to quantify the average total pixels for GFAP+ cells or the presence of CSPG within the lesion site extracellular environment.

also displayed the lowest survival rate over the course of eight weeks suggesting that higher local rolipram dosages could subsequently lead to higher levels of rolipram in the spinal cord and/or body, which could ultimately prove detrimental to the overall health [40–42]. Patches without rolipram proved only slightly advantageous when compared to the no treatment case, thus demonstrating the need to incorporate additional therapeutic agents.

With respect to previous studies, these results suggest that by delivering a low dosage of rolipram directly into the spinal cord, we are able to achieve comparable outcomes with less than 1% of total rolipram delivered (over the course of 3 days). Interestingly, we've also shown that a higher dosage of rolipram directly into the spinal cord (still less than 1% of previous studies), may cause some local toxicity (less recovery within spinal cord) as well as systemic toxicity (increased animal death and weight loss). Because the total amount of rolipram delivered to animals is dramatically less than previous studies, we posit that the apparent variations in outcomes after systemic delivery of rolipram (e.g., via osmotic mini-pumps implanted s.c.) may be due to variations in the amount of drug that enters into the CNS through the blood–brain barrier and injury site.
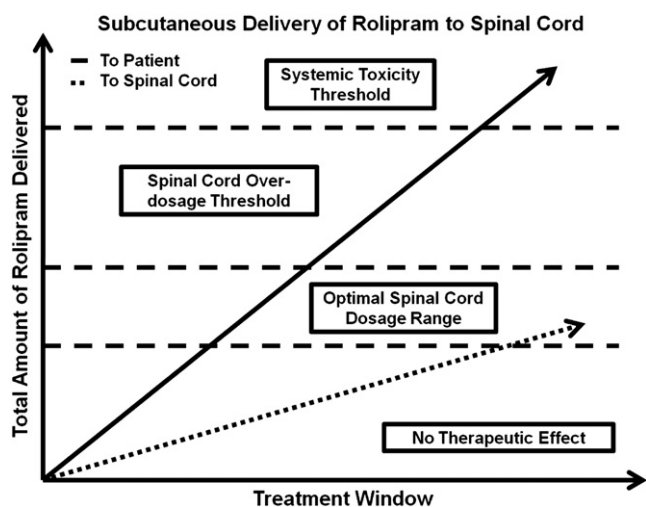
It is important to note that unlike other rolipram related SCI studies, our model utilizes athymic animals. Several other SCI studies have used similar models to help promote the acceptance of xenogenic donor cells after transplantation. Because many of our previous and future studies aim to understand the combined effects of drug-delivery, fibrous scaffolds, and human stem cell transplantation on neural regeneration, an athymic animal model was chosen for clear comparison. This study suggests that drug-eluting microfibrous patches, through a local drug-delivery approach, have the ability to more clearly distinguish optimal and sub-optimal drug dosages for spinal cord repair. In order to further improve recovery and to more thoroughly study the effects of combination therapies on spinal cord repair, future studies will aim to explore the combined delivery of rolipram with other therapeutic agents (i.e., other drugs and/or cells) in addition to creating a more bioactive, cell adhesive hydrogel layer. Release-kinetics will be further improved through additional modifications aimed to enhance hydrogel stability on microfibrous membranes—through the use of various crosslinkers [34] and functional chemistry—thus, preventing rapid hydrogel erosion and delamination.

## 5. Conclusion

This study demonstrates the potential of drug-eluting microfibrous patches as a drug-delivery platform for the local release of rolipram into the injured spinal cord. Here we distinguish the therapeutic outcomes observed from the subdural implantation of patches loaded with low and high doses of rolipram. Patches loaded with lower concentrations yielded significant improvements in functional and anatomical recovery. With increasing loading concentration both functional and anatomical improvements diminished and overall animal health worsened. In all, this study demonstrates the therapeutic utility of drug-eluting microfibrous patches in the study and repair of SCI.

Supplementary data related to this article can be found online at http://dx.doi.org/10.1016/j.jconrel.2012.05.034.

**Fig. 7.** A schematic illustrating the complex balance involved in the s.c. delivery of rolipram to the injured spinal cord for repair. Because only a fraction of the total amount of rolipram delivered s.c. to the patient will reach the spinal cord, systemic rolipram concentrations reach unnecessarily high levels, increasing toxicity related risks. In addition, injury-to-injury and/or patient-to-patient variations can cause uncertainty in the local concentration of rolipram within the spinal cord. As we have shown, inappropriate local concentrations of rolipram within the spinal cord can be detrimental to regeneration. Much of the uncertainty in local spinal cord and systemic rolipram concentrations can be removed with the local delivery of rolipram via drug-eluting microfibrous patches.

## Acknowledgments

## References

[1] One Degree of Separation | Paralysis and Spinal Cord Injury in the United States, Reeve Foundation, 2009, pp. 1–28.
[2] M.T. Fitch, J. Silver, CNS injury, glial scars, and inflammation: inhibitory extracellular matrices and regeneration failure, Exp. Neurol. 209 (2008) 294–301.
[3] T. GrandPre, F. Nakamura, T. Vartanian, S.M. Strittmatter, Identification of the Nogo inhibitor of axon regeneration as a Reticulon protein, Nature 403 (2000) 439–444.
[4] G. Mukhopadhyay, P. Doherty, F.S. Walsh, P.R. Crocker, M.T. Filbin, A novel role for myelin-associated glycoprotein as an inhibitor of axonal regeneration, Neuron 13 (1994) 757–767.
[5] B.P. Niederost, D.R. Zimmermann, M.E. Schwab, C.E. Bandtlow, Bovine CNS myelin contains neurite growth-inhibitory activity associated with chondroitin sulfate proteoglycans, J. Neurosci. 19 (1999) 8979–8989.
[6] L.C. Smith-Thomas, J. Stevens, J. Fok-Seang, A. Faissner, J.H. Rogers, J.W. Fawcett, Increased axon regeneration in astrocytes grown in the presence of proteoglycan synthesis inhibitors, J. Cell Sci. 108 (Pt 3) (1995) 1307–1315.
[7] S. Thuret, L.D. Moon, F.H. Gage, Therapeutic interventions after spinal cord injury, Nat. Rev. Neurosci. 7 (2006) 628–643.
[8] G. Yiu, Z. He, Glial inhibition of CNS axon regeneration, Nat. Rev. Neurosci. 7 (2006) 617–627.
[9] M.E. Schwab, Repairing the injured spinal cord, Science 295 (2002) 1029–1031.
[10] D.C. Baptiste, M.G. Fehlings, Emerging drugs for spinal cord injury, Expert Opin. Emerg. Drugs 13 (2008) 63–80.
[11] J. Zhu, E. Mix, B. Winblad, The antidepressant and antiinflammatory effects of rolipram in the central nervous system, CNS Drug Rev. 7 (2001) 387–398.
[12] D.E. Griswold, E.F. Webb, J. Breton, J.R. White, P.J. Marshall, T.J. Torphy, Effect of selective phosphodiesterase type IV inhibitor, rolipram, on fluid and cellular phases of inflammatory response, Inflammation 17 (1993) 333–344.
[13] D.D. Pearse, F.C. Pereira, A.E. Marcillo, M.L. Bates, Y.A. Berrocal, M.T. Filbin, M.B. Bunge, cAMP and Schwann cells promote axonal growth and functional recovery after spinal cord injury, Nat. Med. 10 (2004) 610–616.
[14] E. Nikulina, J.L. Tidwell, H.N. Dai, B.S. Bregman, M.T. Filbin, The phosphodiesterase inhibitor rolipram delivered after a spinal cord lesion promotes axonal regeneration and functional recovery, Proc. Natl. Acad. Sci. U. S. A. 101 (2004) 8786–8790.
[15] C.A. Iannotti, M. Clark, K.P. Horn, N. van Rooijen, J. Silver, M.P. Steinmetz, A combination immunomodulatory treatment promotes neuroprotection and locomotor recovery after contusion SCI, Exp. Neurol. 230 (2011) 3–15.
[16] C.M. Whitaker, E. Beaumont, M.J. Wells, D.S. Magnuson, M. Hetman, S.M. Onifer, Rolipram attenuates acute oligodendrocyte death in the adult rat ventrolateral funiculus following contusive cervical spinal cord injury, Neurosci. Lett. 438 (2008) 200–204.
[17] E. Beaumont, C.M. Whitaker, D.A. Burke, M. Hetman, S.M. Onifer, Effects of rolipram on adult rat oligodendrocytes and functional recovery after contusive cervical spinal cord injury, Neuroscience 163 (2009) 985–990.
[18] G.C. Koopmans, R. Deumens, A. Buss, L. Geoghegan, A.M. Myint, W.H. Honig, N. Kern, E.A. Joosten, J. Noth, G.A. Brook, Acute rolipram/thalidomide treatment improves tissue sparing and locomotion after experimental spinal cord injury, Exp. Neurol. 216 (2009) 490–498.
[19] K.G. Sharp, L.A. Flanagan, K.M. Yee, O. Steward, A re-assessment of a combinatorial treatment involving Schwann cell transplants and elevation of cyclic AMP on recovery of motor function following thoracic spinal cord injury in rats, Exp. Neurol. 233 (2012) 625–644.
[20] Y.S. Nout, E. Culp, M.H. Schmidt, C.A. Tovar, C. Proschel, M. Mayer-Proschel, M.D. Noble, M.S. Beattie, J.C. Bresnahan, Glial restricted precursor cell transplant with cyclic adenosine monophosphate improved some autonomic functions but resulted in a reduced graft size after spinal cord contusion injury in rats, Exp. Neurol. 227 (2011) 159–171.
[21] Y.D. Teng, E.B. Lavik, X. Qu, K.I. Park, J. Ourednik, D. Zurakowski, R. Langer, E.Y. Snyder, Functional recovery following traumatic spinal cord injury mediated by a unique polymer scaffold seeded with neural stem cells, Proc. Natl. Acad. Sci. U. S. A. 99 (2002) 3024–3029.
[22] V.M. Tysseling-Mattiace, V. Sahni, K.L. Niece, D. Birch, C. Czeisler, M.G. Fehlings, S.I. Stupp, J.A. Kessler, Self-assembling nanofibers inhibit glial scar formation and promote axon elongation after spinal cord injury, J. Neurosci. 28 (2008) 3814–3823.
[23] M. Oudega, S.E. Gautier, P. Chapon, M. Fragoso, M.L. Bates, J.M. Parel, M.B. Bunge, Axonal regeneration into Schwann cell grafts within resorbable poly(alpha-hydroxyacid) guidance channels in the adult rat spinal cord, Biomaterials 22 (2001) 1125–1136.
[24] J.A. Friedman, A.J. Windebank, M.J. Moore, R.J. Spinner, B.L. Currier, M.J. Yaszemski, Biodegradable polymer grafts for surgical repair of the injured spinal cord, Neurosurgery 51 (2002) 742–751 (discussion 751-742).
[25] S. Patel, K. Kurpinski, R. Quigley, H. Gao, B.S. Hsiao, M.M. Poo, S. Li, Bioactive nanofibers: synergistic effects of nanotopography and chemical signaling on cell guidance, Nano Lett. 7 (2007) 2122–2128.
[26] A. Wang, Z. Tang, I.-H. Park, Y. Zhu, S. Patel, G.Q. Daley, S. Li, Induced pluripotent stem cells for neural tissue engineering, Biomaterials 32 (2011) 5023–5032.
[27] Y. Zhu, A. Wang, S. Patel, K. Kurpinski, E. Diao, X. Bao, G. Kwong, W.L. Young, S. Li, Engineering bi-layer nanofibrous conduits for peripheral nerve regeneration, Tissue Eng. Part C Methods 17 (2011) 705–715.
[28] A.J. Wang, Q. Ao, Y.J. Wei, K. Gong, X.S. Liu, N.N. Zhao, Y.D. Gong, X.F. Zhang, Physical properties and biocompatibility of a porous chitosan-based fiber-reinforced conduit for nerve regeneration, Biotechnol. Lett. 29 (2007) 1697–1702.
[29] A.J. Wang, Q. Ao, W.L. Cao, M.Z. Yu, Q. He, L.J. Kong, L. Zhang, Y.D. Gong, X.F. Zhang, Porous chitosan tubular scaffolds with knitted outer wall and controllable inner structure for nerve tissue engineering, J. Biomed. Mater. Res. A 79A (2006) 36–46.
[30] N.S. Adzick, E.A. Thom, C.Y. Spong, J.W. Brock 3rd, P.K. Burrows, M.P. Johnson, L.J. Howell, J.A. Farrell, M.E. Dabrowiak, L.N. Sutton, N. Gupta, N.B. Tulipan, M.E. D'Alton, D.L. Farmer, A randomized trial of prenatal versus postnatal repair of myelomeningocele, N. Engl. J. Med. 364 (2011) 993–1004.
[31] Y.Q. Zhu, A.J. Wang, W.Q. Shen, S. Patel, R. Zhang, W.L. Young, S. Li, Nanofibrous patches for spinal cord regeneration, Adv. Funct. Mater. 20 (2010) 1433–1440.
[32] P. Saadai, Y.S. Nout, J. Encinas, A. Wang, T.L. Downing, M.S. Beattie, J.C. Bresnahan, S. Li, D.L. Farmer, Prenatal repair of myelomeningocele with aligned nanofibrous scaffolds—a pilot study in sheep, J. Pediatr. Surg. 46 (2011) 2279–2283.
[33] C.K. Hashi, Y. Zhu, G.Y. Yang, W.L. Young, B.S. Hsiao, K. Wang, B. Chu, S. Li, Anti-thrombogenic property of bone marrow mesenchymal stem cells in nanofibrous vascular grafts, Proc. Natl. Acad. Sci. U. S. A. 104 (2007) 11915–11920.
[34] H.H. Tonnesen, J. Karlsen, Alginate in drug delivery systems, Drug Dev. Ind. Pharm. 28 (2002) 621–630.
[35] M. Martinez, J.M. Brezun, L. Bonnier, C. Xerri, A new rating scale for open-field evaluation of behavioral recovery after cervical spinal cord injury in rats, J. Neurotrauma 26 (2009) 1043–1053.
[36] D.M. Basso, M.S. Beattie, J.C. Bresnahan, A sensitive and reliable locomotor rating scale for open field testing in rats, J. Neurotrauma 12 (1995) 1–21.
[37] Kelli G. Sharp, Lisa A. Flanagan, Kelly Matsudaira Yee, Oswald Steward, A re-assessment of a combinatorial treatment involving Schwann cell transplants and elevation of cyclic AMP on recovery of motor function following thoracic spinal cord injury in rats, Exp. Neurol. 233 (2) (2012) 625–644.
[38] S.M. Willerth, S.E. Sakiyama-Elbert, Approaches to neural tissue engineering using scaffolds for drug delivery, Adv. Drug Deliv. Rev. 59 (2007) 325–338.
[39] S. Kajana, H.G. Goshgarian, Administration of phosphodiesterase inhibitors and an adenosine A1 receptor antagonist induces phrenic nerve recovery in high cervical spinal cord injured rats, Exp. Neurol. 210 (2008) 671–680.
[40] H. Wachtel, Potential antidepressant activity of rolipram and other selective cyclic adenosine 3′,5′-monophosphate phosphodiesterase inhibitors, Neuropharmacology 22 (1983) 267–272.
[41] H. Wachtel, H.H. Schneider, Rolipram, a novel antidepressant drug, reverses the hypothermia and hypokinesia of monoamine-depleted mice by an action beyond postsynaptic monoamine receptors, Neuropharmacology 25 (1986) 1119–1126.
[42] G.F. Hebenstreit, K. Fellerer, K. Fichte, G. Fischer, N. Geyer, U. Meya, M. Sastre-y-Hernández, W. Schöny, M. Schratzer, W. Soukop, E. Trampitsch, S. Varosanec, E. Zawada, R. Zöchling, Rolipram in major depressive disorder: results of a double-blind comparative study with imipramine, Pharmacopsychiatry 22 (1989) 156–160.